Russian Journal of Electrochemistry, Vol. 40, No. 7, 2004, pp. 736–742. Translated from Elektrokhimiya, Vol. 40, No. 7, 2004, pp. 843–851.

Electrolytic Iron Sulfide Products in Lithium Batteries

E. M. Shembel'[a,b,z], R. D. Apostolova[b], V. M. Nagirnyi[a,b], A. S. Baskevich[b], and P. M. Litvin[c]

[a] *Ener 1, Ft Lauderdale, 33309 Florida, USA*
[b] *Ukrainian State University of Chemical Technology, pr. Gagarina 8, Dnepropetrovsk, 49005 Ukraine*
[c] *Institute of Semiconductor Physics, National Academy of Sciences of Ukraine, pr. Nauki 45, Kiev, 03028 Ukraine*

Received August 6, 2003; in final form, October 8, 2003

Abstract—A technology for electrolytic production of iron sulfide compounds applicable in thin-layer lithium batteries is developed. Physicochemical and structural properties and the surface morphology of compounds are studied by x-ray diffraction and thermal analyses, absorption IR spectroscopy, and atomic force microscopy. Specific discharge characteristics of compounds in thin-layer compact nonballast and paste electrodes of model lithium power sources are determined. The discharge capacity of compounds in thin layers weighing 1.0–7.5 mg cm^{-2} galvanostatically cycled in electrolyte PC, DME, 1 M $LiClO_4$ at room temperature stays at 200–320 mA h g^{-1} for 40–50 cycles.

Key words: pyrite, iron sulfides, lithium battery, discharge, charge, electrolytic synthesis

INTRODUCTION

Natural and synthetic pyrite, which is used in primary lithium power sources, is a best candidate for cathodic materials of rechargeable batteries for electric vehicles. The coulombic efficiency of the pyrite cycling is high in high-temperature lithium batteries with eutectic LiCl–KCl [1, 2] and medium-temperature batteries with a solid polymer electrolyte [3, 4]. Pyrite can undergo reversible electrochemical conversion at room temperature in gel, hybrid, and polymer electrolytes [5, 6]. In liquid aprotic electrolytes, only a small fraction of the theoretical specific energy of natural pyrite is realized when cycling an FeS_2/Li system paired with a solar cell [7]. Physicochemical properties of iron sulfides can be altered by polarization in aqueous media [8]. The pyrite structure may be stabilized by electrochemically doping it with metals [9].

In connection with this, electrolysis was used as a means for synthesizing compounds containing iron sulfides (COCIS) suitable for lithium batteries operating at room temperature in liquid aprotic electrolytes [10]. An optimum balance of COCIS in synthesis products may guarantee effective electrochemical energy conversion. One of the two goals of using electrolysis was the formation of thin compact COCIS layers of weight 1.0–7.5 mg cm^{-2} on a conductive substrate as well as COCIS in the form of finely divided powders used in the paste electrodes containing ballast additives of a conductive component and a binder. The other was the activation of pyrite—the preparation of composite mixtures of COCIS and powders co-deposited from a suspension of pyrite in the deposition electrolyte.

Here we synthesize COCIS suitable for thin-layer lithium batteries with a liquid electrolyte operating at low temperatures. The pyrite activation by means of an electrolysis will be described later.

EXPERIMENTAL

The physicochemical and structural properties and the morphology of synthesized COCIS were examined by x-ray diffraction (XRD) and thermal analyses, absorption IR spectroscopy, atomic force microscopy (AFM), and profilometry. Electrochemical characteristics of COCIS were determined galvanostatically in a discharge–charge process in a model lithium battery.

The XRD patterns for powdered or compact COCIS on stainless steel and aluminum were recorded on a DRON-2.0 setup (35 kV, 20 mA) using single-crystal LiF as the monochromator and CoK_α radiation. The intensity was measured at $2\theta = 10°$–$80°$. The IR general absorption spectra for powdered COCIS were obtained on a 75IR spectrophotometer (Specord) at wave numbers of 4000–500 cm^{-1}. The matrix was KBr of ultrahigh purity grade. Derivatograms for powdered COCIS were taken on a Q-1500 D derivatograph when heating at 10 degrees per minute. To determine the relief and thickness of COCIS, we recorded profiles of the COCIS surface on a DEKTAK 3030 profilometer

[z] Corresponding author, e-mail: eshembel@ener1.com or shembel@onil.dp.ua

(Germany). The morphology of the COCIS surface was studied using a Nanoscope 111a atomic force microscope (Digital Instruments). The measurements were taken in a regime of periodic contact of silicon probes of the NT-MDT firm (Russia) of the NSG01 brand (ultrasharp noncontact "Golden" silicon cantilevers) with a curvature radius of 10 nm and the pyramidal probe height of 10–20 nm. The specific discharge characteristics of COCIS were studied at room temperature in model lithium sources size 2325 with thin-layer nonballast and composite cathodes (with addition of acetylene black and a polytetrafluoroethylene binder, 10% each), manufactured using technology [11].

In anodes of the models we used lithium plates of an excess weight ~1.5 mm thick, 16 mm in diameter. The models were filled with a nonaqueous electrolyte 1 M $LiClO_4$ ($LiClO_4$—Iodobrom, Saki, Ukraine), PC, DME (propylene carbonate—Angarsk shop of chemicals, dimethoxyethane—Merck), the latter in the 1 : 3 volume ratio. The models were assembled in a glove box filled with dry argon and galvanostatically cycled at 3.5–1.1 and 1.8–0.1 V on a test stand at discharge current densities I_d = 25–280 mA g^{-1}.

RESULTS AND DISCUSSION

The active electrode material (COCIS) was obtained in the form of compact thin layers (1.0–7.5 mg cm^{-2}) by a cathodic deposition on plates or gauzes of stainless steel (18Kh12N10T) or aluminum alloy (AMG-6) the size of 10 by 10 by 0.3 mm and also on a bottom inner surface of a stainless-steel body of a button power source 2325. To obtain finely powdered COCIS we used plates of technical titanium (VT-1) with an area of 10 cm^2.

Preparation of the AMG-6 substrate surface included its etching in an NaOH solution (200 g l^{-1}) and bleaching in H_2SO_4 (150–200 g l^{-1}); and that of 18Kh12N10T and VT-1, the polishing with an abrasive and pickling in a mixture of H_2SO_4, HCl, and HNO_3. Subsequent washing of the substrates with distilled water preceded the cathodic deposition of COCIS in an electrolyte (pH 4.0–5.0), which contained, in g l^{-1}: $FeSO_4$, 7.5–10.0; $CuSO_4$, 0.50–0.55; $NiSO_4$, 1.0–1.5; and $Na_2S_2O_3$, 3.5–5.0. This composition was optimum for obtaining homogeneous compact mechanically stable deposits with a high enough electrochemical activity. The anodes were VT-1 plates. The ratio of the cathodes' area to that of the anodes' ranged from 1–5 to 1–10. The electrolysis was run at I_c = 1.5–2.5 mA cm^{-2} and 20–25°C, in a thermostated glass cell (250 cm^3). Its duration was determined by the specified deposit weight and deposition rate (2.5–4.5 mg cm^{-2} h^{-1}). The synthesis having terminated, the obtained electrolytic deposits (e-COCIS) were washed with distilled water and dried at 180 or 250–300°C (7 h) or at room temperature (15–24 h) in air or in a vacuum.

The mechanism of the effect of additives (nickel and copper sulfates) is not yet clear, but when taken in the above amounts they increase stability and workability of the electrolyte. Some XRD patterns for cathodic deposits exhibited reflexes corresponding to NiS. Copper ions may induce the formation of chalcogenides of the type $CuFeS_2$ on the cathode. These accompanying compounds probably influence positively the balance of cathodic material. Additives may hinder iron hydration in the near-cathode layer, forming instead labile metal hydroxides, which may accelerate interaction of iron ions with sulfur.

Electrochemical processes that may occur during electrolysis are represented by reactions

$$S_2O_3^{2-} + 6H^+ + 8e \longleftrightarrow 2S^{2-} + 3H_2O \quad E^0 = -0.006\ \text{V}, \quad (1)$$

$$S_2O_3^{2-} + 6H^+ + 4e \longleftrightarrow 2S + 3H_2O \quad E^0 = +0.465\ \text{V}, \quad (2)$$

$$S^{2-} + H^+ \longleftrightarrow HS^- \quad E^0 = -0.65\ \text{V}, \quad (3)$$

$$2Fe(OH)_2 + 2HS^- + 2H^+ \longleftrightarrow 2FeS + 4H_2O, \quad (4)$$

$$Fe^{2+} + 2S + 2e \longleftrightarrow FeS_2 \quad E^0 = +0.34\ \text{V}, \quad (5)$$

$$2Fe^{3+} + 3S^{2-} \longleftrightarrow Fe_2S_3, \quad (6)$$

$$FeS + S_2O_3^{2-} \longleftrightarrow FeS_2 + SO_3^{2-}, \quad (7)$$

which are only conjectural and are presented here in an attempt to explain XRD-identified iron sulfide compounds. Having summarized by one of reactions (2)–(5), we have

$$S_2O_3^{2-} + Fe^{2+} + 6H^+ + 6e \longleftrightarrow FeS_2 + 3H_2O. \quad (8)$$

Compact e-COCIS comprise dark brown, dark gray, or black layers. The AFM images of deposits on steel and aluminum hardly differ in nanomorphology. The deposits form grains (200–300 nm) displaying growth steps or layers. On aluminum, e-COCIS are less rough (Figs. 1c, 1d) than on stainless steel (Figs. 1a, 1b). The average size of grainy formations on aluminum is smaller than on steel. Subgrains form macrograins only on steel, which is clearly seen in the 5 by 5 μm scans.

From a profilogram for e-COCIS of a weight of 1.8 mg cm^{-2} and an area of 1.44 cm^2 we determined thicknesses of an active electrolytic stratum. The average density of the deposit, according to profilometry, is 4.1 g cm^{-3}. The density of e-COCIS deposited from electrolyte with the Fe : S ratio of 10.0 to 3.5 and dried at 180°C for 10 h, determined with a pycnometer and dimethylformamide as the standard, is 4.84 g cm^{-3}; its porosity is 17%.

According to the XRD patterns (Fig. 2), e-COCIS are multiphase systems whose composition depends on the synthesis conditions. Results of an XRD analysis of deposits given in Fig. 2 are listed in Table 1.

The electrolytic deposits are finely divided, crystalline. The crystallite size L, determined from the peaks with spacings of 0.271, 0.285, and 0.202 nm for FeS_2

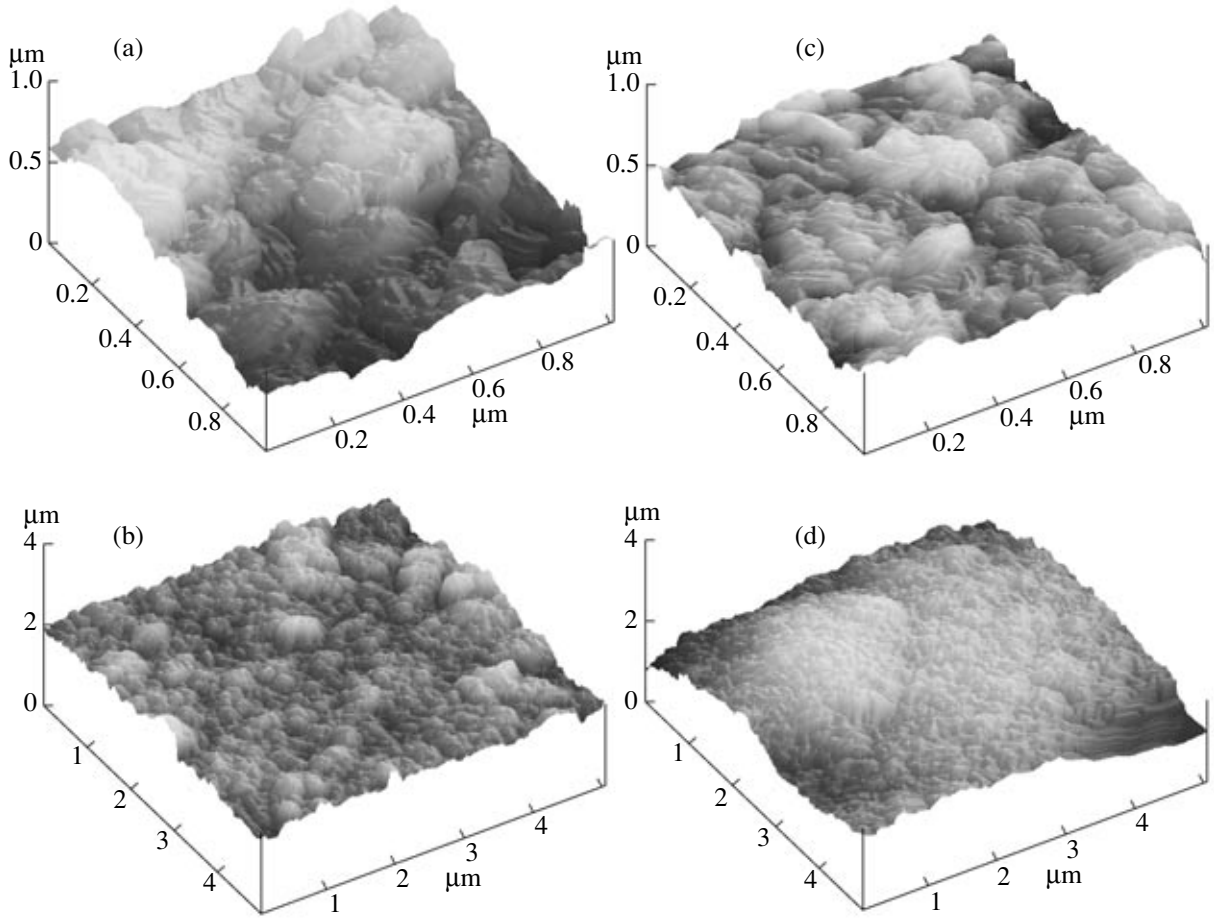

Fig. 1. AFM images of e-COCIS surface on (a, b) steel (1.8 mg cm^{-2}) and (c, d) aluminum (3.7 mg cm^{-2}).

(pyrite), FeS, and Fe_3S_4 by an approximation method [12] is 12–64 nm. The basic components of these deposits are iron sulfides; also present are iron oxides and sulfur. In the electrolyte containing nickel and copper ions, tiny amounts of sulfides of nickel or copper oxide could form. Qualitative and quantitative balance between components in e-COCIS depends on the balance between $FeSO_4$ and $Na_2S_2O_3$ (Fe : S) in electrolyte. At high contents of thiosulfate ions (Fe : S = 3 : 1), iron ions interact faster with sulfide ions formed in (1)–(3), accelerating the formation of sulfides (50–75%) FeS_2 or Fe_2S_3. The interaction is also facilitated by enhanced migration into the near-cathode layer of ions of iron of higher valence (III, IV), which form on the anode. A decrease in the relative content of thiosulfate ions in electrolyte and the surface concentration of sulfide ions on the cathode probably causes the formation of iron forms less saturated by sulfide (for the 4 : 1 ratio of Fe to S). The cathodic process may also be affected by such factors as the oxidation of Fe(II) on the anode and the partial formation of free sulfur in electrolyte as a result of the decomposition of thiosulfate ions.

The composition of thin-layer deposits depends on the substrate material. In identical synthesis conditions, e-COCIS on steel consisted of FeS, γ-Fe_2O_3, and S, whereas the deposit on aluminum comprised Fe_3S_4,

Table 1. XRD results for e-COCIS (Fig. 2)

Sample no.	Fe : S electrolyte	Deposit composition	*L*, nm	Sample no.	Fe : S electrolyte	Deposit composition	*L*, nm
1	4 : 1	FeS, FeS_2 (pyrite), S	22.0	4	10.0 : 3.5	FeS_2(pyrite), γ-Fe_2O_3	24.4
2	3.0 : 1.5	FeS_2 (pyrite), FeS_2 (marcasite), γ-Fe_2O_3	18.5	5	10 : 5	Fe_3S_4, γ-Fe_2O_3	20.3
3	4 : 1	FeS, S	37.0				

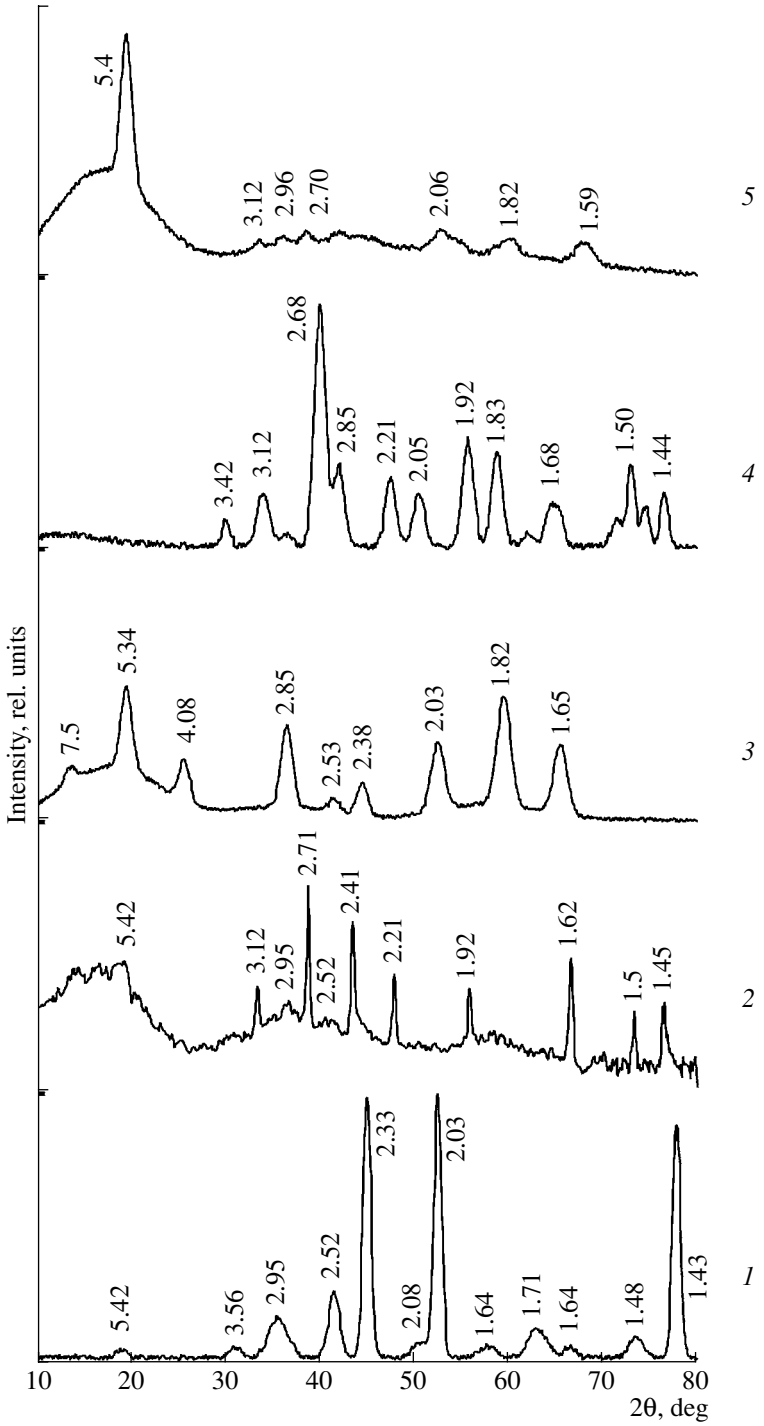

Fig. 2. XRD patterns for e-COCIS composed of (*1*) FeS, FeS_2 (pyrite), S; (*2*) FeS_2 (pyrite), FeS_2 (marcasite), γ-Fe_2O_3; (*3*) FeS, S; (*4*) FeS_2 (pyrite), γ-Fe_2O_3; and (*5*) Fe_3O_4, γ-Fe_2O_3.

γ-Fe_2O_3, and FeS. This difference may be due to partial influence of a contact deposition of aluminum at the instance of loading the aluminum cathode. The chemical composition of e-COCIS depends also on the after-electrolysis treatment: on whether they were dried in air or in a vacuum at room temperature. For example, e-COCIS deposited from electrolyte with the 4 : 1 ratio of Fe to Ni and dried in air consists of FeS, S, and γ-Fe, while that dried in a vacuum comprises FeS, FeS_2 (pyrite), and S.

The IR absorption spectra for e-COCIS at 400–4000 cm^{-1} indicate the presence of compounds accompanying sulfides. The spectra for e-COCIS synthesized from electrolytes with the Fe : S : Ni ratios equal to 4 : 1 : 0.1 and 3 : 1 : 0.13 clearly display only absorption

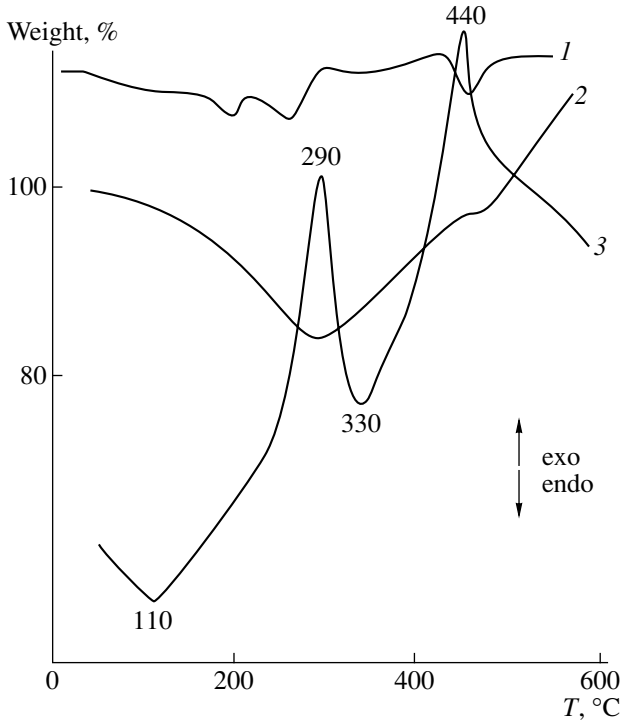

Fig. 3. (*1*) DTG, (*2*) TG, and (*3*) DTA curves for e-COCIS deposited from electrolyte with the Fe : Ni : S ratio of 7.5 : 1.0 : 5.0; numbers near curve *3* refer to temperature in °C.

bands belonging to bonds of water coordinated in the form of molecules and OH^- groups (1622, 3436 cm^{-1}). The smeared low-intensity absorption bands with maximums at 1230, 1110, 1010, and 590 cm^{-1} refer to vibrations of bonds of sulfate ions [13] captured by the deposit from electrolyte and testify that these are hardly present in e-COCIS. Reflexes of sulfide bonds occur below 400 cm^{-1} and will be analyzed individually.

The derivatogram for e-COCIS synthesized from electrolyte with the Fe : S : Ni ratio of 7.5 : 5.0 : 1.0 (Fig. 3) reflects thermochemical instability of a multiphase system at 50–500°C. Conversely, natural pyrite is stable in this temperature interval [14]. Thermogravometric curves for e-COCIS exhibit several steps of the loss and the gain of weight. In the DTA curves the

Table 2. Endo- and exothermic effects of samples

Sample no.	Sample	Endoeffect				Exoeffect	
		1	2	3	4	1	2
1	Fe : S : Ni 7.5 : 5 : 1	110		330		290	440
2	Fe : S : Ni 4 : 1 : 0.1	100		310	460	310	410
3	FeS_2 (synthetic)	100	170	330	490	290	360
4	S	96.119	164				

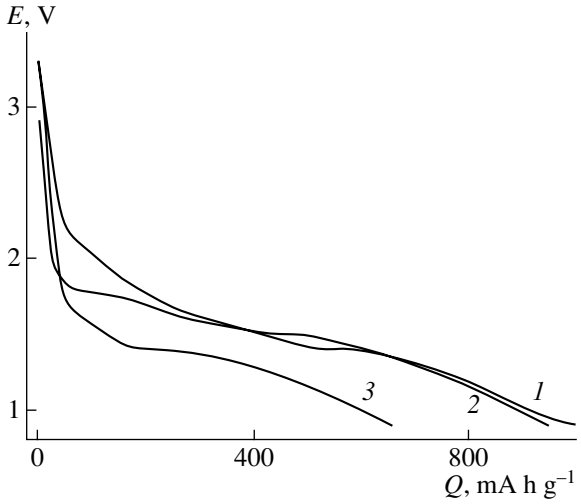

Fig. 4. Discharge curves for [FeS, FeS_2 (pyrite), S]/Li with paste electrodes in the 1st cycle; electrode drying temperature is (*1*) 18, (*2*) 180, and (*3*) 250°C; active mass weight is 12 mg cm^{-2}, I_d = 0.1 mA cm^{-2}.

endothermic effects overlap the exothermic effects, suggesting that the composition of e-COCIS alters when heated. Derivatograms for e-COCIS deposited from electrolytes with the Fe : S ratios equal to 7.5 : 5.0 and 4.0 : 1.0 differ. Table 2 compares maximums of endothermic and exothermic effects in e-COCIS with those in sulfur and synthetic pyrite. Synthetic nanostructural pyrite is as thermally unstable as nanostructural e-COCIS. The DTA data show that the e-COCIS composition may be altered by heat.

The open-circuit voltage for e-COCIS/PC, DME, 1 M $LiClO_4$/Li is 3.0–3.2 V. Samples of e-COCIS may be electrochemically active as cathodic materials for 1.5-volt lithium power sources (Figs. 4, 7–9) and as anodic materials of lithium-ion batteries—below 1.0 V relative to Li (Fig. 5). The results of a galvanostatic cycling of e-COCIS at 3.5–1.1 V are presented below.

The composition FeS, FeS_2 (pyrite), S was studied in models with the paste and nonballast electrodes. With the paste electrodes, its discharge capacity in the first cycle is 650–950 mA h g^{-1} (depending on the drying temperature) and rises in the temperature series 250 < 180 < 18°C (Fig. 4). The reversible capacity is 210–220 mA h g^{-1} (40th cycle, Fig. 6b). These values exceed the discharge capacity of an analogue with the paste electrodes based on synthetic pyrite (0.5–5.0 μm fraction), which provides 40 mA h g^{-1} in the 17th cycle (Fig. 6c). With nonballast thin-layer electrodes, the discharge capacity of this composition in the first cycle is as high as that with the paste electrodes and reaches 300 mA h g^{-1} in the 40th cycle (Fig. 6a), while the reversible capacity exceeds that in the paste electrodes.

When cycling the composition FeS_2 (pyrite), FeS_2 (marcasite), γ-Fe_2O_3, deposited on aluminum as thin layers weighing 1.5–2.0 mg cm^{-2}, the discharge capac-

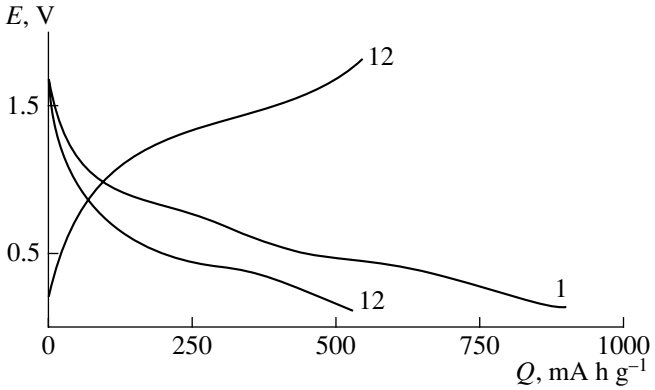

Fig. 5. Discharge–charge profile for [FeS, FeS_2 (pyrite), S]/Li; weight 1.5 mg cm^{-2}, I_d = 33 mA g^{-1}. Figures near curves denote cycle numbers.

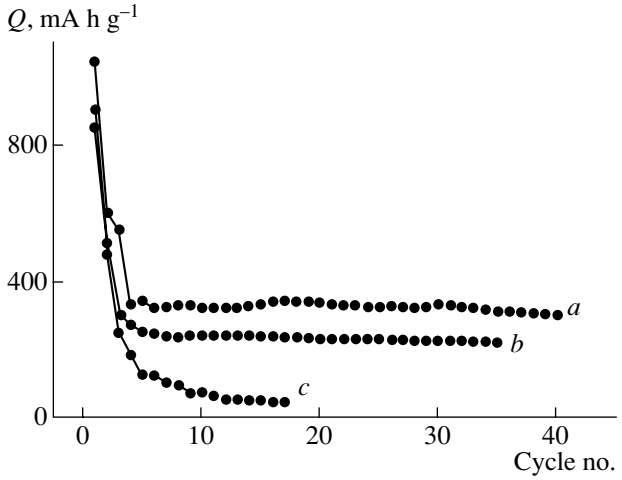

Fig. 6. Discharge capacity for (*a*) nonballast and (*b, c*) paste electrodes composed of (*a, b*) FeS, FeS_2 (pyrite), S and (*c*) nanostructural synthetic pyrite; active weight of electrodes is (*a*) 1.4, (*b*) 12, and (*c*) 13 mg cm^{-2}; discharge currents are (*a*) 0.05, (*b*), (*c*) 0.2 mA cm^{-2}.

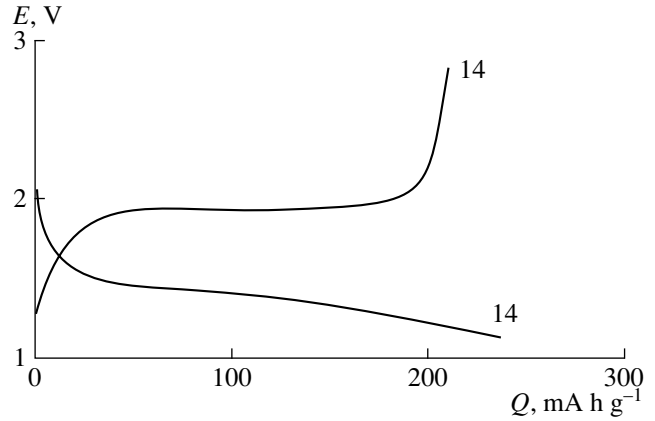

Fig. 7. Discharge–charge profile for [FeS_2 (marcasite), FeS_2 (pyrite), γ-Fe_2O_3]/Li; weight is 1.4 mg cm^{-2}, I_d = 37 mA g^{-1}. Figures near curves denote cycle numbers.

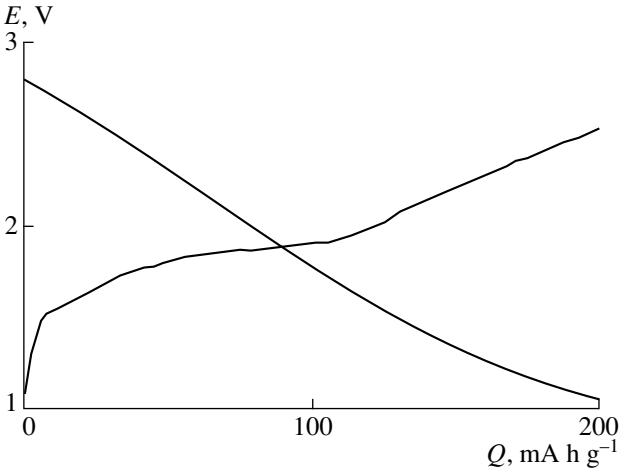

Fig. 8. Discharge–charge profile for [FeS, S, γ-Fe_2O_3]/Li; weight 3.6 mg cm^{-2}, I_d = 280 mA g^{-1}.

ity becomes stable after the sixth cycle and amounts to 225 mA h g^{-1} in the 40th cycle. The discharge–charge profile of the 14th cycle is shown in Fig. 7.

The discharge capacity of the composition FeS, γ-Fe_2O_3, S, deposited on aluminum, in models is equal to 925 and 250 mA h g^{-1} in the 1st and 40th cycles (I_d = 30 mA g^{-1}). The discharge–charge profile remains invariant for ten cycles at I_d = 280 mA g^{-1} (Fig. 8), with the discharge capacity reaching 200 mA h g^{-1}.

The discharge profile of e-COCIS for the first cycle in many cases exhibits two horizontally-slanted portions of voltage of 2.0–1.65 and 1.60–1.40 V (Fig. 4). Discharge profiles for the 1st and 2nd cycles differ, suggesting that the phase composition of e-COCIS alters after the first discharge. The discharge profile of e-COCIS may be "corrected" to obtain a profile ideal for a power source, which has one horizontal plateau of voltage. For example, a correction was done by adding a calculated amount of sucrose in the form of a solution into the deposition electrolyte. Figure 9 shows the discharge–charge profile for a model with thin-layer e-COCIS deposited in the presence of sucrose. The discharge plateau of modified e-COCIS in the first cycle corresponds to a voltage of 1.4 V, which remains practically invariant for a few cycles.

CONCLUSIONS

A cathodic reduction of aqueous acid solutions containing iron sulfides may lead to the formation of compounds capable of a reversible electrochemical conversion in lithium batteries with a liquid electrolyte at

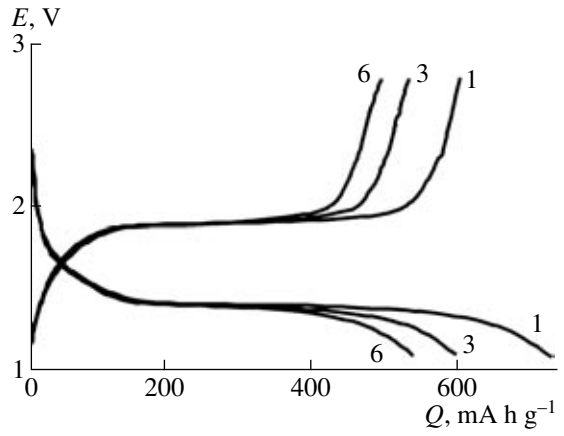

Fig. 9. Discharge–charge curves for e-COCIS deposited from electrolyte containing sucrose (0.5 g l^{-1}) in model power source with nonballast electrodes; active mass weight is 2.0 mg cm^{-2}, I_d = 25 mA g^{-1}. Figures near curves denote cycle numbers.

room temperature. The synthesized product can include FeS_2, FeS, γ-Fe_2O_3, sulfur, and impurities, whose quantitative balance depends on the electrolyte composition, electrolysis parameters, and the thermal treatment of the deposits. Ions of nickel and copper in the electrolyte improve the adhesion of compact deposits to the substrate and specific discharge characteristics of synthesized electrode materials. Characteristics of e-COCIS can effectively be modified by additives in the electrolyte.

According to the XRD and AFM data, the synthesized e-COCIS material is nanostructural. Nanostructural materials possess peculiarities due to their large surface areas. This tells in a certain manner on the electrochemical processes in such materials. For example, the electrochemical intercalation of lithium ions in nanostructural synthetic pyrite is a heterogeneous process [15] proceeding both on the surface and in the bulk of the solid phase, whereas in natural pyrite with the particle size of 5–15 μm the electrochemical conversion occurs predominantly in the bulk via some other mechanism.

The production of nonballast e-COCIS electrodes gives a chance of using them in real rechargeable thin-layer batteries, which are in increasing demand due to miniaturization of power sources for portable communication instruments, electronics, etc. Hence, optimizing the thickness of e-COCIS for economically advantageous rechargeable lithium batteries warrants further investigation.

ACKNOWLEDGMENTS

This work was supported by the Ener 1 company, contract no. USO-1207, and UNTTs, contract no. 1810.

REFERENCES

1. Pleto, S.K., Tomczuk, Z., von Winbusch, S., and Roche, M.F., *J. Electrochem. Soc.*, 1983, vol. 130, p. 264.
2. Clark, M.B., *Littium Batteries*, Gabano, J.P., Ed., New York: Academic, 1983, p. 115.
3. Strauss, E., Golodnitsky, D., and Peled, E., *Electrochim. Acta*, 2000, vol. 45, p. 1519.
4. Kazunori, T., Yoshiro, K., Taro, I., Akihira, K., Masaru, K., Shigeo, K., Mamoru, W., and Mitsuharu, T., *J. Electrochem. Soc.*, 2001, vol. 148, p. 1085.
5. Shembel, E., Chervakov, O., Neduzhko, L., Maksyuta, I.M., Polichuk, Yu.V., Reisner, D.E., Novak, P., and Meshri, D., *J. Power Sources*, 2001, vol. 96, p. 20.
6. Appetecchi, G.B., Romagnoli, P., Scrosati, B., Ardel, G., Golodnitsky, D., and Peled, E., Abstracts of Papers, *1999 Joint Int. Meet., Hawaii, October 17–22, 1999*, no. 366.
7. Apostolova, R. and Shembel', E., *Zh. Prikl. Khim.* (Leningrad), 1995, vol. 68, p. 1483.
8. Chanturiya, V.A. and Wiegderhaus, V.E., *Elektrokhimiya sul'fidov: Teoriya i praktika flotatsii* (The Electrochemistry of Sulfides: Theory and Application of Flotation), Moscow: Nauka, 1993.
9. Abd El Halim, A.M., Fiecher, S., and Tributsch, H., *Electrochim. Acta*, 2002, vol. 47, p. 2615.
10. Shembel, E., Apostolova, R., Nagirny, V., Baskevich, A., Lytvyn, P., and Eskova, N., Abstracts of Papers, *23d Int. Power Sources Symp., September 22–24, 2003.*
11. Shembel, E., Apostolova, R., Nagirny, V., Aurbach, D., and Markovsky, B., *J. Power Sources*, 1999, vol. 80, p. 90.
12. Gorelik, E.S., Skolov, Yu.A., and Rastorguev, L.N., *Rentgenostrukturnyi i elektronno-opticheskii analiz* (The X-Ray and Electron-Optic Analysis), Moscow: MISIS, 1994.
13. Nyquist, R.A. and Kagel, R.O., *Infrared Spectra of Inorganic Compounds*, New York: Academic, 1971.
14. Golodnitsky, D. and Peled, E., *Electrochim. Acta,* 1999, vol. 45, p. 335.
15. Shao-Horn, Y., Osmialowski, S., and Horn, Q.C., *J. Electrochem. Soc.*, 2002, vol. 149, p. 1547.